Amsterdam '09

U024

A Variable Projection Method for Waveform Inversion

T. van Leeuwen* (Delft University of Technology) & W.A. Mulder (Shell International E&P)

SUMMARY

Waveform inversion can be cast into an optimization problem in two parameters: the reflectivity and the background velocity model. The problem is linear with respect to the reflectivity and strongly nonlinear with respect to the background velocity. By resolving the reflectivity via a migration step, the problem can be re-formulated as an optimization problem in one parameter: the background velocity.
With an example we illustrate that this makes the least-squares functional better behaved. It turns out that this functional is most sensitive to differences in amplitude between the observed and predicted data. This may be problematic when the amplitudes of the data are not correctly modelled. We show that a functional based on the correlation of the observed and predicted is mainly sensitive to the phase difference and may circumvent this problem. We include examples on synthetic data computed with finite differences for a 2D velocity model.

Waveform inversion

In waveform inversion, the goal is to obtain a velocity model from seismic data by minimizing the least-squares (LS) error between the observed and predicted data. We may split the velocity model into a reflectivity r and a smooth background velocity c_0. Under the assumptions of the Born approximation, the seismic data can now be modelled as

$$p = F[c_0]r, \tag{1}$$

where F is the linearized modelling operator, depending on the background velocity. Throughout the paper, the data are modelled with a time-domain finite-difference code. Given observed data, the correct model parameters (c_0, r) minimize the LS functional:

$$J_{\text{ls}}[c_0, r] = ||F[c_0]r - p_{\text{obs}}||_2^2. \tag{2}$$

In practice, one employs a gradient-based optimization algorithm to find the model parameters that minimize this. A well-known problem of this approach is that the functional exhibits local minima and has a small basin of attraction around the global minimum. Next, we illustrate these issues with a sensitivity analysis.

Sensitivity analysis

In the Fourier domain, we may represent the data as

$$\hat{p}(\omega, h) = a(\omega, h) \exp\big[\imath\omega\phi(h)\big], \tag{3}$$

where a is the amplitude factor and ϕ is the phase factor. The amplitude factor is mostly sensitive to changes in the reflectivity, while the phase factor is mostly sensitive to changes in the background velocity. We illustrate this by computing data for the velocity model depicted in figure 1(a) and varying the amplitudes of the reflectivity and velocity perturbations. The result is shown in figure 1(c,d) and confirms our earlier statement.

We can investigate the sensitivity of the LS functional to changes in the amplitude and phase of the data by combining equations 2 and 3. Some manipulation yields

$$J_{\text{ls}} = ||a||_2^2 + ||a_{\text{obs}}||_2^2 - 2\int \mathrm{d}h \int \mathrm{d}\omega\, a a_{\text{obs}} \cos\big(\omega\,(\phi(h) - \phi_{\text{obs}}(h))\big). \tag{4}$$

Figure 2 depicts the behaviour of the functional to changes in the amplitude and phase for a low and a high frequency, and a stack over frequencies. This clearly illustrates some well-known issues in waveform inversion: *(i)* both amplitude and phase can be resolved when starting with a single, low frequency, *(ii)* for high frequencies, or even a stack over frequencies, local minima are present and the basin of attraction of the global minimum is very small. From the figure we may conclude that the LS functional is geared towards fitting the amplitudes of the data.

Separable least-squares problems

An efficient way to solve inverse problems like the one stated above is the *variable projection* algorithm (Kaufman, 1975). The idea is to eliminate the linear parameter, in this case the reflectivity, by means of the normal equations:

$$r[c_0] = (F^*[c_0]F[c_0])^{-1}F^*[c_0]p_{\text{obs}}, \tag{5}$$

where F^* denotes the adjoint or migration operator. The above can be interpreted as a true-amplitude migration of the data, given the background velocity model c_0. Substituting this into equation 2 yields a modified LS functional that only depends on the background velocity:

$$\tilde{J}_{\text{ls}}[c_0] = ||(F[c_0](F[c_0]^*F[c_0])^{-1}F[c_0]^* - I)p_{\text{obs}}||_2^2. \tag{6}$$

Here, $(F(F^*F)^{-1}F^* - I)$ projects p_{obs} onto the null space of F. Hence the name, variable projection algorithm. A very similar approach is Migration Based Traveltime inversion, proposed by Clément *et al.* (2001). In practice, computing the exact projection is too costly since it involves computing the Hessian. We will neglect the Hessian and use just $\alpha \cdot FF^*$ as projector, where α is a scalar factor that minimizes $\tilde{J}_{\text{ls}}$.

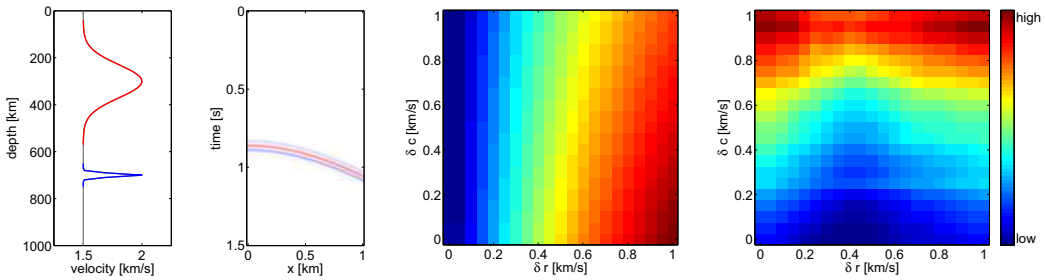

Figure 1: (a) velocity (red) and reflectivity (blue) perturbation superimposed on a constant velocity. (b) Corresponding data. Norm of the (a) amplitude and (b) phase of the data for different amplitudes of the velocity and reflectivity perturbations.

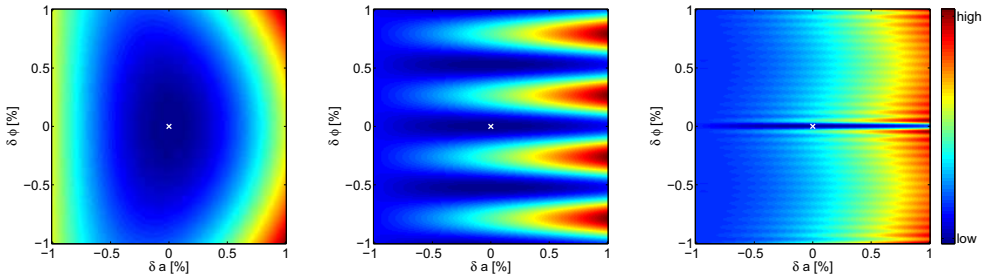

Figure 2: Sensitivity of the least-squares functional (equation 2) to changes in the amplitude and phase of the data for: (a) 0.1 Hz, (b) 2 Hz and (c) a stack over frequencies from $2-15$ Hz. The global minimum is indicated with a cross.

Example on model-consistent data

We present an example for the 2D Synclay velocity model depicted in figure 3. This model is adapted from Clément *et al.* (2001) and is continued as a 1D layered model outside the range $0-1000$ m. A total of 41 shots where simulated with a spacing of 50 meters, starting at $x = -1000$ m. Each shot contains 41 traces with offsets ranging from 0 to 1000. A shot record of the corresponding constant-density acoustic data is depicted in the same figure. Next, we introduce a velocity perturbation, shown in figure 3(b), and study the projection and the functional for varying amplitude of this perturbation. Figure 4 displays the result of the projection operator applied to the data. Finally, the behaviour of the functional is presented in figure 6(a). The LS functional is a stack over the LS differences for each shot.

Example on non-model-consistent data

It is more relevant to consider data that is not model-consistent. We compute variable-density data for the Synclay model, where the density is calculated according to Gardner's rule. For the projection of the data we use a constant density model. This leads to an amplitude difference between the 'observed' data and the predicted data for the correct velocity model. The behaviour of the functional is depicted in figure 6(b). This shows that the functional does not attain a minimum for the correct velocity model. We have concluded earlier that the functional is geared towards fitting the amplitudes of the data. However, the amplitudes of the observed and predicted data are not the same for the correct velocity model, causing the minimum to be in the wrong place.

A different functional

The above examples showed that when relying on the amplitudes to obtain the correct velocity model they have to be model-consistent. Even a difference in density models makes the method break down. The phases of the data, on the other hand, are mainly sensitive to changes in the background velocity.

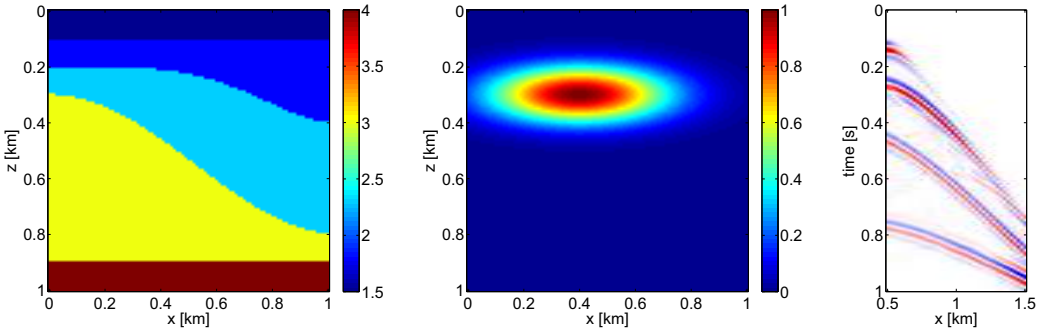

Figure 3: (a) Synclay velocity model, (b) velocity perturbation, (c) synthetic shot record at $x = 500$ m.

Therefore, we would like to use a functional that is more sensitive to differences between the phases of the observed and predicted data. In an earlier paper (van Leeuwen and Mulder, 2008a) we introduced a functional that is based on the correlation of the observed and predicted data. This correlation responds to phase differences by focusing, as is illustrated in figure 5. The corresponding functional is given by

$$J_h[c_0] = ||W_\gamma \cdot C[p, p_{\text{obs}}]||_2^2, \tag{7}$$

where $p = \alpha F[c_0]F^*[c_0]p_{\text{obs}}$, $C[p,q](t,\Delta h) = \int \mathrm{d}h\, p(t,h)q(t,h+\Delta h)$ and $W_\gamma(\Delta h) = \exp(-\gamma \Delta h^2)$. This functional measures the amount of energy concentrated around zero shift, where γ determines the width of the area around zero shift. For the correct velocity model, this attains a maximum. This functional is evaluated for each shot and then stacked. The behaviour of the functional for the 2D example is depicted in figure 6(c). It shows that maximizing the correlation-based functional will lead to the correct velocity model, even if the amplitudes are not modelled correctly.

Conclusion

In this paper we explained how the variable projection method can be applied to waveform inversion. With some examples we illustrate that this approach relies on fitting the amplitudes of the data to find the correct background velocity. This causes the method to break down in case the amplitudes are not model consistent. In earlier work we introduced an alternative functional which exploits the correlation of the observed and predicted data. This functional is more sensitive to phase differences and attains a maximum for the correct velocity model, even if the amplitudes are not modelled correctly. This approach proved successful in the context of the convolutional model (van Leeuwen and Mulder, 2008a) and has been applied to finite difference modelling for 1D velocity models (van Leeuwen and Mulder, 2008b). We illustrate here that there is no inherent limitation to the method and that it can be applied to laterally varying velocity models.

Acknowledgments

This work is part of the research programme of the 'Stichting voor Fundamenteel Onderzoek der Materie (FOM)', which is financially supported by the 'Nederlandse Organisatie voor Wetenschappelijk Onderzoek (NWO)'.

References

Clément, F., Chavent, G., and Gómez, S. [2001] Migration-based traveltime waveform inversion of 2-D simple structures: A synthetic example. *Geophysics* 66(3), 845–860.

Kaufman, L. [1975] A variable projection method for solving separable nonlinear least squares problems. *SIAM Journal of Numerical Analysis* 15–49.

van Leeuwen, T., and Mulder, W.A. [2008a] Velocity analysis based on data correlation. *Geophysical Prospecting* 56(6).

van Leeuwen, T., and Mulder, W.A. [2008b] Waveform inversion with data correlation. *EAGE Extended abstracts*.

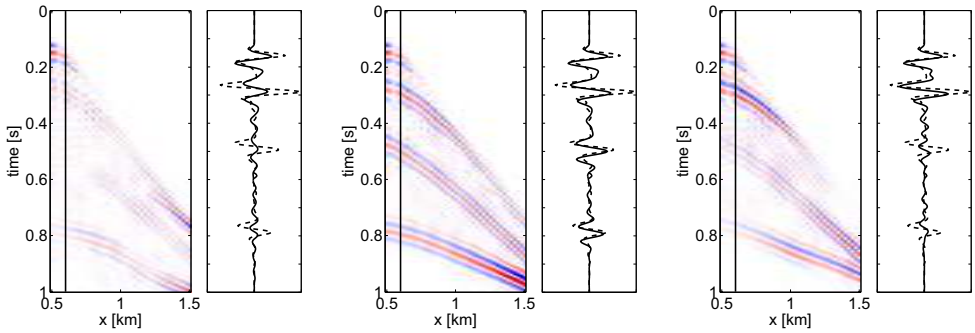

(a) (b) (c)

Figure 4: Projection of a shot record (figure 3(c)) for different amplitudes of the velocity perturbation (figure 3(b)): (a) -1 km/s, (b) 0 km/s and (c) 1 km/s. The dashed traces are the observed ones, the solid traces are the projections.

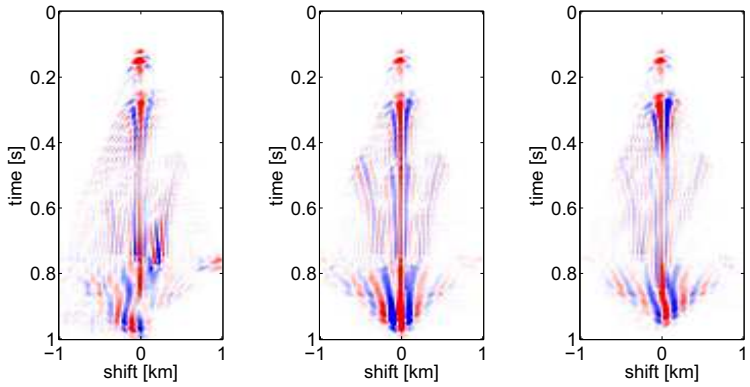

(a) (b) (c)

Figure 5: Correlation of observed and projected data for different amplitudes of the velocity perturbation: (a) -1 km/s, (b) 0 km/s and (c) 1 km/s. The focussing can best be observed around .9 s.

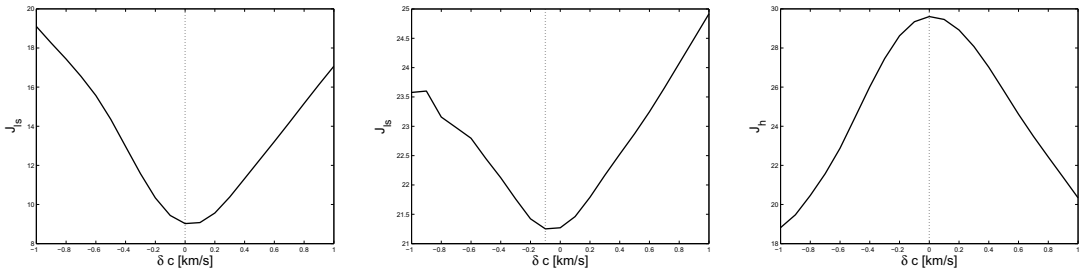

(a) (b) (c)

Figure 6: Functionals as function of the amplitude of the velocity perturbation. (a) Least-squares functional for model consistent data, (b) LS functional for variable-density data, (c) correlation-based functional for variable density data. The dashed line indicates the position of the extremum.